THE EFFECT OF INTERACTION LAWS ON THE STRESSES IN FRICTIONLESS GRANULAR MEDIA

S. LUDING,[a] H.-G. MATUTTIS
Institute for Computer Applications 1, Pfaffenwaldring 27, 70569 Stuttgart, Germany

We simulate static model sandpiles in two dimensions (2D) and focus on the stresses inside the pile. In this study tangential forces, e.g. friction, are neglected. We compare the simplest possible interaction model, i.e. a linear spring and a linear dashpot, with a nonlinear law based on Hertz' theory. Furthermore, we present data obtained by a simulation of frictionless polygons with twelve sides also placed on a triangular lattice. The stresses depend only slightly on the choice of either interaction law or particle shape.

1 Introduction

One out of many interesting features of granulates [1] is the stress distribution in static arrays of sand. The pressure in a silo filled with grains does not increase linearly with depth as in the case of a liquid filling. Instead, the stress saturates at a certain value [2] due to arching and internal friction. Thus the walls of the silo carry a part of the materials' weight. In a pile of sand where no vertical walls are present the total weight of the pile is carried by the bottom. However, the distribution of forces under and inside the material is not yet completely understood. Experiments on piles with many thousands of particles reveal a relative minimum in the vertical stress at the bottom of the pile, the so-called dip.[3,4] In the presence of disorder, stress chains are observed, i.e. stresses are mainly transported along selected paths, and the probability distribution of stress spans several orders of magnitude.[5,6,7]

From simple sandpile models, like arrays of rigid particles,[8,9] the stress at the bottom of the pile is calculated to be constant in contrast to experimental observations. A continuum approach may lead to a dip in the vertical stress if certain assumptions for the constitutive equations are chosen.[10] Also a lattice model [11] shows the dip in average over many realizations.

The simplest model granular material, i.e. particles in 2D interacting via linear springs without friction, includes most of the above mentioned findings as special cases.[7] Here, we extend the simple linear interaction law [7], to a more realistic nonlinear contact law based on the elastic theory by Hertz,[12] and check how the results differ. Finally, we compare the different interaction laws with a simulation using polygonal particles.[13]

2 Simulation Aspects

In the simulations N particles with diameter $d_0 = 1.5$ mm are used. In the lowermost layer, $M = 0$, at the bottom we place L immobile particles. We model heaps of slope 30^o by adding $L_M = L - 3M$ particles for layer $M = 1, ..., H^{(30)}$ respectively. The number of particles in the pile is thus $N^{(30)} = H^{(30)}(L - 3(H^{(30)} - 1)/2)$ with the number of layers $H^{(30)} = \text{int}[(L-1)/3] + 1$.

[a] e-mail: lui@ica1.uni-stuttgart.de

The initial velocities and overlaps of the particles are set to zero, and gravity is slowly tuned from zero to the selected magnitude and the system is simulated until the kinetic energy is several orders of magnutide smaller than the potential energy.

For the relaxation of the array we use a standard molecular dynamics (MD) procedure with a fifth order predictor-corrector scheme.[14] Since we are interested here in static arrangements of particles in the gravitational field, we use strong viscous damping, in order to reach the steady state quickly. The MD method is not the best choice for a fast relaxation, however, closing and opening of contacts is implemented straightforwardly.

There are two forces acting on particle i when it overlaps with particle j, i.e. when the distance $r_{ij} =\mid \vec{r}_j - \vec{r}_i \mid \leq (d_i + d_j)/2$. We use an elastic force

$$\vec{f}_{el}^{(i)} = -k_e((1/2)(d_i + d_j) - r_{ij})^{(1+e_1)}\vec{n}_{ij}, \tag{1}$$

with the spring constant k_e, acting on particle i in normal direction $\vec{n}_{ij} = (\vec{r}_j - \vec{r}_i)/r_{ij}$. The second force in normal direction is dissipative

$$\vec{f}_{diss}^{(i)} = \mu_e(\vec{v}_{ij} \cdot \vec{n}_{ij})((1/2)(d_i + d_j) - r_{ij})^{e_2}\vec{n}_{ij}, \tag{2}$$

accounting for the inelasticity of the contacts. The contact of a particle with an immobile particle is mimicked by setting the mass of the immobile contact partner to infinity. In Eq. 2 the constant μ_e is a phenomenological dissipation coefficient, and $\vec{v}_{ij} = \vec{v}_j - \vec{v}_i$ is the relative velocity of the particles i and j. Note that the nonlinear powers e_1 and e_2 is not neccessarily the same in Eqs. 1 and 2, however, we restrict ourselves to $e = e_1 = e_2 = 0$ or $e = 1/2$. The simple linear spring-dashpot model corresponds to e=0, and the nonlinear Hertz law for spheres,[15] together with the damping proposed by Kuwabara and Kono,[16] corresponds to $e = 1/2$. Furthermore, we present some data from simulations of polygonal particles and mark those with $e = 1$. The simulation method for polygons is outlined elsewhere. [13] The power $e = 1$ is consistent with the interaction law obtained for the edge of a polygon hitting a side of another polygon.

The quantity we discuss in the following is the stress tensor σ,[17,18] which we identify in the static case with

$$\sigma_{\alpha\beta}^{(i)} = (1/V^{(i)})\Sigma\ s_\alpha f_\beta, \tag{3}$$

where the indices α and β indicate the coordinates, i.e. x and z in 2D. This stress tensor is an average over all contacts of the particles within volume $V^{(i)}$, with the distance s between the center of the particle and the contact point, and the force f acting at the contact point.

From a relaxed configuration of particles we calculate the components of the stress tensor $\sigma_{xx}, \sigma_{zz}, \sigma_{xz}$, and σ_{zx} and define $\sigma^+ = (\sigma_{xx} + \sigma_{zz})/2$, $\sigma^- = (\sigma_{xx} - \sigma_{zz})/2$, and $\sigma^* = \sigma_{xz}$. If we neglect tangential forces the spherical particles are torque-free and we observe only symmetric stress tensors, i.e. $\sigma_{zx} = \sigma_{xz}$. The eigenvalues of σ are thus $\sigma_{\max,\min} = \sigma^+ \pm \sqrt{(\sigma^-)^2 + (\sigma^*)^2}$, and the major eigenvalue is tilted counterclockwise by an angle

$$\phi = \arctan\left(\frac{\sigma_{\max} - \sigma_{xx}}{\sigma_{xz}}\right) \tag{4}$$

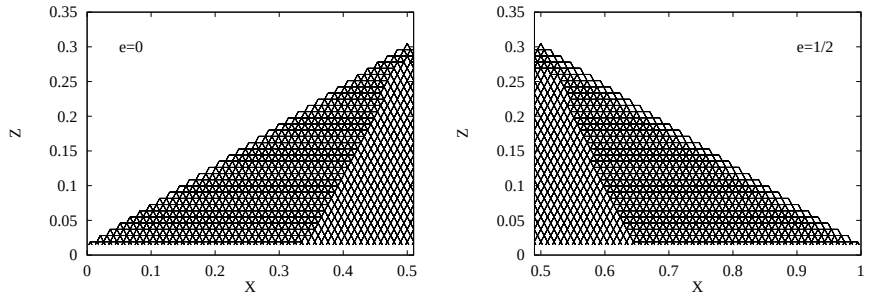

Figure 1: Half views of the contact network for simulations with linear (left) and nonlinear (right) interaction laws.

from the horizontal. Throughout this study we use the dimensionless stress $S = 2\sigma/(\rho g h) = \sigma l/(mg)$ with the density ρ, the mass of the pile m, the width of the pile l, and the height of the pile h. With this scaling, the sum over the vertical stresses at the bottom $S_{zz}(1)$ gets unity. Furthermore, we use dimensionless coordinates $X = x/l$ and $Z = z/l$ in horizontal and vertical direction respectively.

3 Comparison of different interaction laws

The situation we address is a homogeneous pile, as assumed in Ref.[7] Here we use $L_0 = 100$ particles in row $M = 0$ and create a 30^o pile. The particles in the lowermost row $M = 0$ are fixed with horizontal separation d_0.

In Fig. 1 we compare the contact network for the two interaction laws defined above. The piles with linear interaction, i.e. $e = 0$, and nonlinear interaction, i.e. $e = 1/2$, are presented as the left and right half-pile respectively. We observe a triangular region with diamond-lattice contact network in the center of the pile and a triangular contact network at the shoulders. Only in a thin layer close to the surface we find a diamond-lattice tilted outwards from the center. The structure, i.e. the contact network is the same for both interaction laws, except for some weak deviations.

In Fig. 2a we plot the components of the dimensionless stress tensor $S(1)$ versus $X = x/l$ for the lowermost row of mobile particles, $M = 1$. From bottom to top we plot the components S_{xz}, S_{xx}, and S_{zz}. Besides small deviations the stress tensor is the same in all cases $e = 0$, $e = 1/2$, and $e = 1$. The ratios of stresses, i.e. S_{xz}/S_{zz} and S_{xx}/S_{zz} are plotted in Fig. 2b and we observe that the ratio of the diagonal elements is about $1/3$ inside the pile, independently from e. The value of $1/3$ is consistent with the theoretical predictions in Ref.[10] for a 60^o diamond structure inside a 30^o pile and can also be understood from geometrical arguments: Since the horizontal contact is open, the stiffness of the material is weaker in horizontal direction than in vertical direction for a 60^o diamond-lattice. In horizontal direction we find a contribution to the stiffness $k_e \cos 60^o$ on a vertical length $d_0 \sin 60^o$. On the other hand, in vertical direction we find a contribution to the stiffness of $k_e \cos 30^o$ on a horizontal length $d_0 \sin 30^o$. Assuming a homogeneous deformation we arrive at $S_{xx}/S_{zz} = \tan^2 30^o = 1/3$.

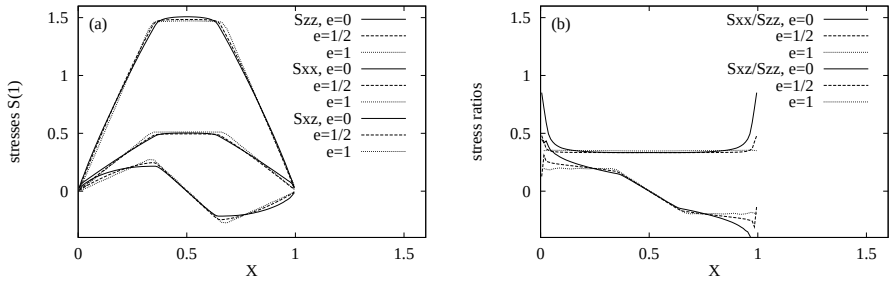

Figure 2: (a) Components of the dimensionless stress tensor $S(1)$ at row $M = 1$ vs. dimensionless horizontal coordinate $X = x/l$, for a pile with immobile particles at the bottom, $M = 0$. The slope of the pile is 30^o and $L_1 = 97$. We use linear $e = 0$, and nonlinear interactions $e = 1/2$, see insert. The data with $e = 1$ correspond to simulations with polygonal particles. (b) Ratios of the components of $S(1)$ presented in (a) for the corresponding simulations.

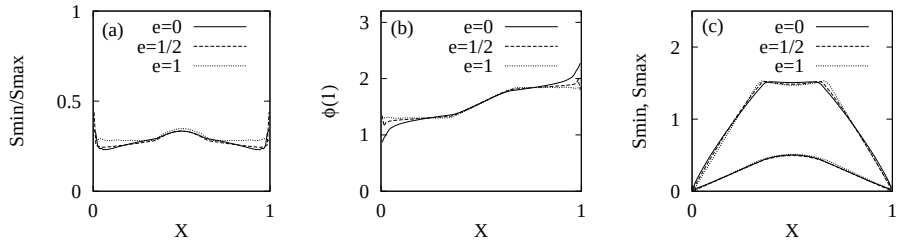

Figure 3: (a) Ratio of the eigenvalues of the stress tensor at row $M = 1$ vs. X, for the piles from Fig. 2. (b) The angle ϕ about which the major principal axis is tilted from the horizontal in counterclockwise direction. (c) The minor and major eigenvalues $S_{\min}$ and $S_{\max}$.

From the stress tensor S in cartesian coordinates we move now into the principal axis system, where S is defined by the minor and major Eigenvalues $S_{\min}$ and $S_{\max}$ and the angle of orientation ϕ as defined in Eq. 4. We plot the ratio of the eigenvalues $S_{\min}/S_{\max}$ in Fig. 3a, the angle $\phi(1)$ in Fig. 3b, and the minor and major eigenvalues in Fig. 3c. Except for boundary effects close to $X = 0$ and $X = 1$ we have three regions which may be identified as the regions with different contact network in Fig. 1. In the center the stresses are almost constant and decrease at the outer part of the pile until they vanish at the boundary. Except for the center, the stress tensor is always oriented outwards from the center. The orientation angle ϕ is almost constant in the outer regions and a transition takes place in the inner region.

4 Summary and Conclusion

We presented simulations of particles arranged as a pile in 2D with a slope of 30^o and measure the stresses inside the pile for different interaction laws. We compare the simple linear spring $e = 0$, with a non-linear spring $e = 1/2$ (based on the elastic theory by Hertz), and with polygonal particles $e = 1$. We observe that the qualitative behavior is almost independent of the interaction law used. The contact

network, i.e. the fabric or the structure of the pile, is seemingly more important than the specific interaction law between the particles. The nonlinearity – connected to the opening and closing of contacts – determines the qualitative behavior of the stresses in the situation presented here.

In our simplified model without friction we do not observe arching or stress chains as long as no fluctuations are introduced.[7] With fluctuations in the order of a few percent of the particle size, the behavior of the system gets much more complex. In future more detailed studies with friction should be performed and the sensitivity of the stress distribution on the construction history should be tested.

Acknowledgements

We thank J. D. Goddard, H. J. Herrmann, and J. J. Wittmer for helpful discussions, and acknowledge the support of the European network "Human Capital and Mobility" and of the DFG, SFB 382 (A6).

References

1. H. M. Jaeger, S. R. Nagel, and R. P. Behringer, *Physics Today* **49**, 32 (1996).
2. H. A. Janssen, *Zeitschr. Vereines deutscher Ingenieure* **XXXIX**, 1045 (1895).
3. D.H. Trollope and B.C. Burman, *Géotechnique* **30**, 137 (1980).
4. J. Smid and J. Novosad, *I. Chem. E. Symposium Series* **63** D3/V/1 (1981).
5. C. h. Liu, S. R. Nagel, D. A. Schecter, S. N. Coppersmith, S. Majumdar, O. Narayan, and T. A. Witten, *Science* **269**, 513 (1995).
6. F. Radjai, M. Jean, J. J. Moreau, and S. Roux, *Phys. Rev. Lett.* **77**, 274 (1996).
7. S. Luding, preprint 1997.
8. K. Liffman, D.Y.C. Chan, and B.D. Hughes, *Powder Technology* **72**, 255 (1992).
9. D.C. Hong, *Phys. Rev.* E **47**, 760 (1993).
10. J.P. Wittmer, M.E. Cates, and P. Claudin, *J. Phys. I (France)* (1996).
11. J. Hemmingsson, H. J. Herrmann, and S. Roux, preprint 1996.
12. L. Landau and E. Lifschitz, *Elasticity Theory*, (MIR, Moscow, 1967).
13. H.-G. Matuttis and S. Luding, this volume.
14. M. P. Allen and D. J. Tildesley, *Computer Simulation of Liquids*, (Oxford University Press, Oxford, 1987).
15. S. Luding *et al.*, *Phys. Rev.* E **50**, 4113 (1994).
16. G. Kuwabara and K. Kono, *Japanese Journal of Applied Physics* **26**, 1230 (1987).
17. J. D. Goddard, p. 179 in Pitman Research Notes in Mathematics No. 143, (Longman/J. Wiley, New York, 1986).
18. R.J. Bathurst and L. Rothenburg, *J. Appl. Mech.* **55**, 17 (1988).